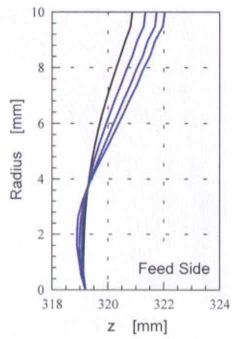

(f) 1 g

Fig. 9 Time Evolutions of Interface Shapes at Feed Side (Red Line: Every 2 Hours)

In order to obtain a single crystal, it is important that not only the interface shape but also the degree of supercooling. Therefore, the degree of the supercooling is investigated and is shown in Fig. 10. In 0 g case, the supercooling region can hardly be observed. As the gravity increases, however, the supercooling region occurs around the axis. In the current boundary conditions, the maximum supercooling location is near the feed on axis. Although the allowable value of the supercooling is unknown now, if the degree of the supercooling of less than 0.1 % is assumed to be allowable, the gravity of less than or equal to 10^{-4} g is required. This gravity should be easily achieved by the International Space Station. The degree of supercooling becomes maximal at 1 g, but the value is only about 0.48 %. This is not so large value and may be allowable for suppression of excess nucleation. These results suggests that the current boundary conditions such as the heating condition and the gravity direction are suitable for the suppression of the supercooling.

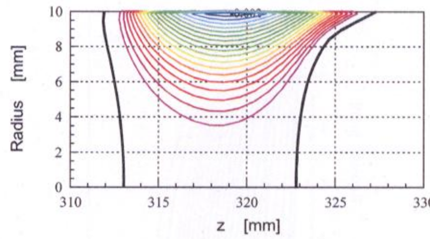

(a) 0 g

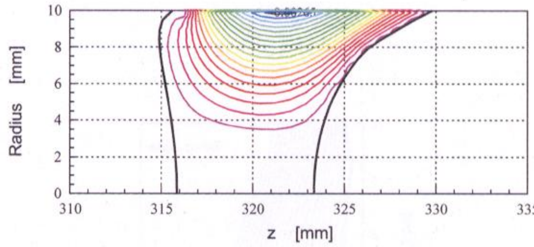

(b) 10^{-5} g

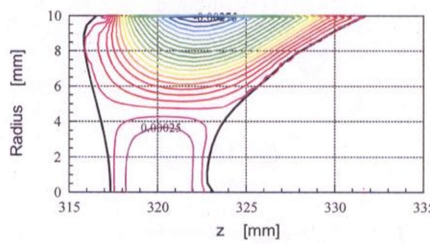

(c) 10^{-4} g

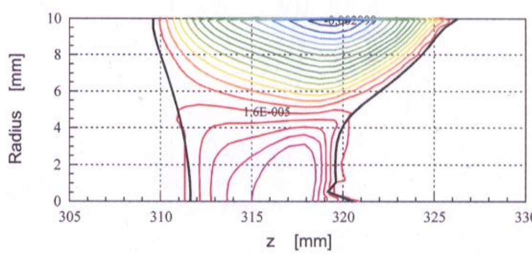

(d) 10^{-2} g

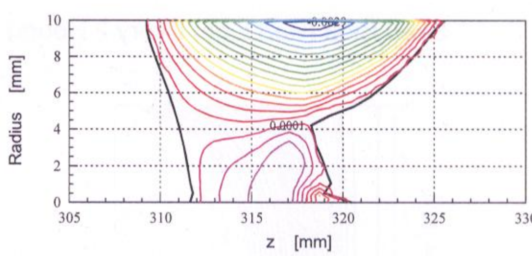

(e) 10^{-1} g

Fig. 10 Distribution of Degree of Supercooling (*Cont.*)

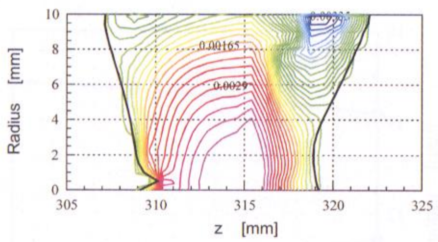

(f) 1 g

Fig. 10 Distribution of Degree of Supercooling

Discussion

The TLZ method has several superiorities as compared with conventional growth methods, that is, (i) spontaneous growth, (ii) robustness against the convection. But there may be limitations for obtaining large and homogeneous crystals. One of the limitations may be the maintenance of the zone width. The zone width may disappear or stretch resulting in the breakdown of the TLZ mode. Figure 11 shows the time evolutions of the zone widths at various gravity levels. In the cases of the low gravity of less than or equal to 10^{-4} g, the width on axis linearly decreases though the width on the wall increases. By extrapolating the data, the time when the zone disappears on axis can be estimated; (a) 4500 min., (b) 3300 min., and (c) 3060 min. depending on gravity level. This disappearance is essential to the TLZ method because the crystal grows as indium in the zone is consumed. The disappearance also means that the growth rate is not the same as the dissolution rate. Namely, the rates are determined independently by satisfying the heat and mass balances at each interface. But the interfaces move just like the synchronized motion as a result. Of course, the time for the zone disappearance depends on the several conditions such as the interface shape, the temperature and the concentration gradients, and the gravity.

In the cases of higher gravity of more than or equal to 10^{-2} g, the behavior is different from the lower gravity cases, that is, the width on axis decreases but the decreasing rate also gradually becomes low, and begins to increase at a certain time. This should be caused by the convection. If this tendency is maintained, the width continues expanding and thus the TLZ mode will fail soon or later. This failure mode may be corresponding to experimental results of the extreme deformation of the interface shape at the feed side.

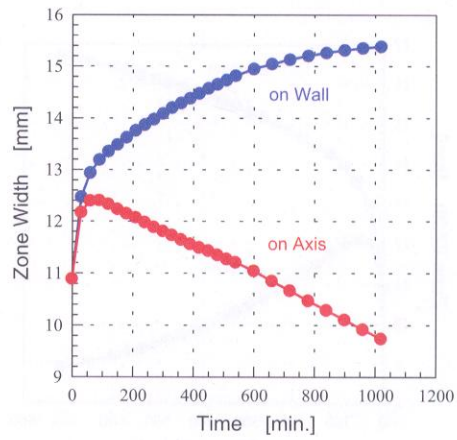

(a) 0 g

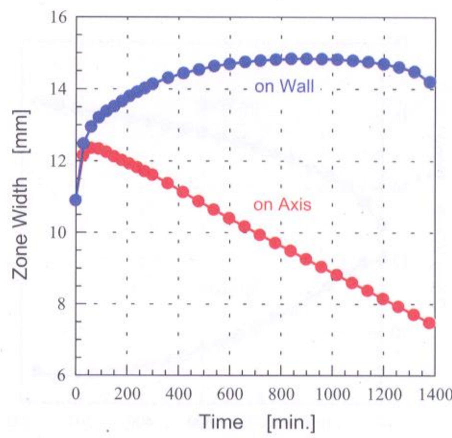

(b) 10^{-5} g

Fig. 11 Time Evolutions of Zone Width (*Cont.*)

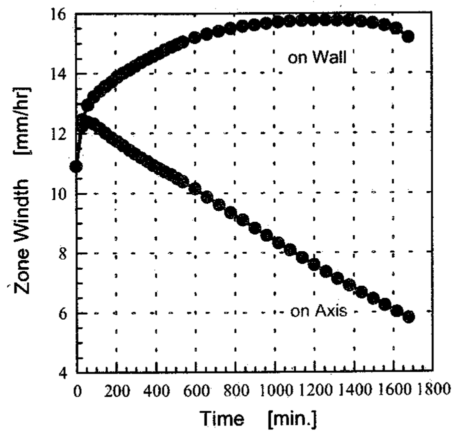

(c) 10^{-4} *g*

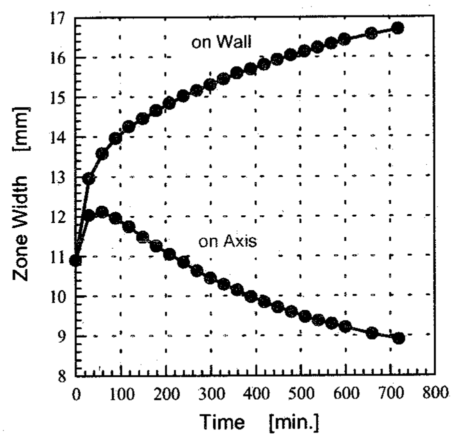

(d) 10^{-2} *g*

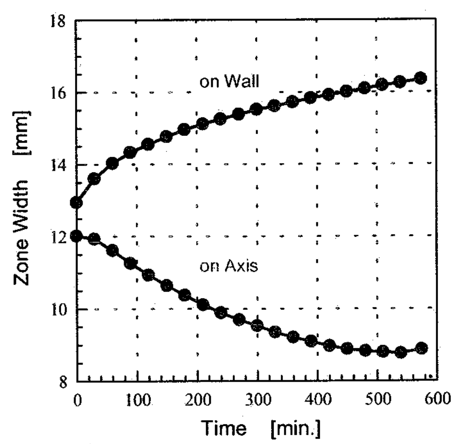

(e) 10^{-1} *g*

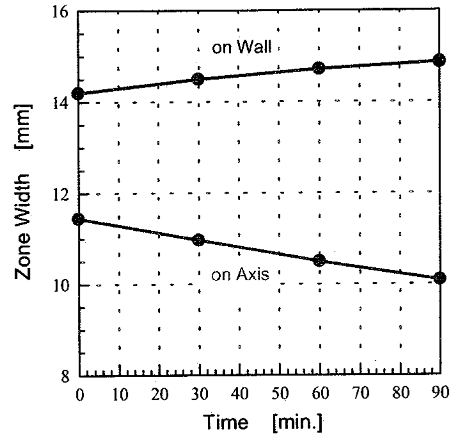

(f) 1 *g*

Fig. 11 Time Evolutions of Zone Width

In order to understand the reason of the behavior difference between at the lower gravities and the higher gravities, the time evolutions of the growth rates are investigated because the width is the result of the change of the growth rate at the seed side and the melting rate at the feed side. These are shown in Fig. 12 and 13. In Fig. 12, the growth rate on axis is nearly constant at the quasi-steady state, that is, 0.36 ± 0.02 mm/hr. The growth rate on the wall is similar to the rate on axis but the quasi-steady state may not be achieved in some cases. For short duration of several hundred minutes, the rate on the wall seems to be steady, but such condition is sometimes broken down. This is not due to the convection because the breakdown can be observed under the lower gravity conditions. Unfortunately the exact reason is not clear, but it should be sure that the width on the wall would not continue spreading under the lower gravity condition, and this should contribute to the sustenance of the TLZ mode.

In Fig. 13, the steady state is also obtained at the lower gravity levels. But the rate at the feed side is smaller than that at the seed side. This is the reason for the width decreasing on axis. The rate at the higher gravity is more difficult to reach the steady state. The required time to become steady should be longer than the time in the lower gravity case at least. This is also caused by the convection. Since the center of the vortex is nearer the feed side than the seed side in the case of less than or equal to 10^{-2} *g*, the convection influence is larger and thus the required time to be steady becomes longer.

By using the typical growth rate and the termination time of the TLZ mode, the growth length can be obtained. The maximum length should be 27 mm at 0 *g*, 19.8 mm at 10^{-5} *g* and 18.4 mm at 10^{-4} *g* under the current boundary conditions. Though this is not so long at the point of view of the absolute value, it is long enough to evaluate the crystal quality and to make a test device of a laser diode. Of course, the maximum length can be easily longer by using the wider solution zone such as the initial value of 15 mm or 20 mm. Although the wider zone makes the maintenance of the TLZ mode more difficult, the microgravity condition will enhances the maintenance capability. In addition, another condition such as a smaller radius sample will also contribute to the longer lifetime of the TLZ mode due to the smaller deformation of the interface shape.

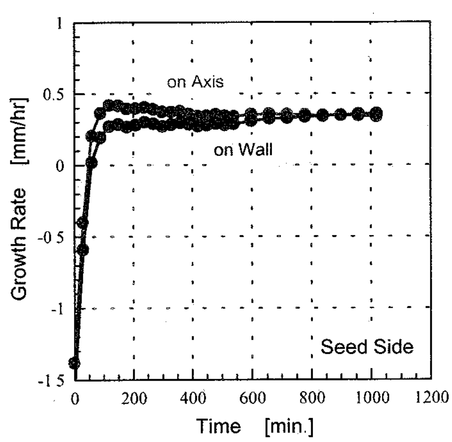

(a) 0 *g*

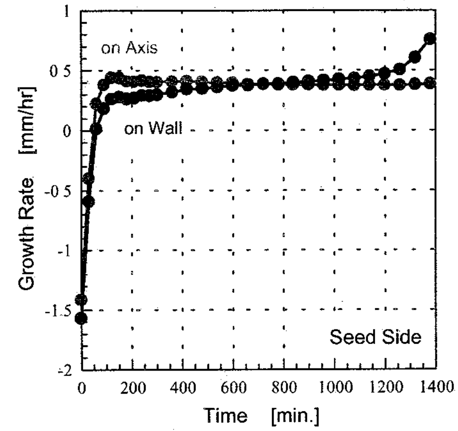

(b) 10^{-5} *g*

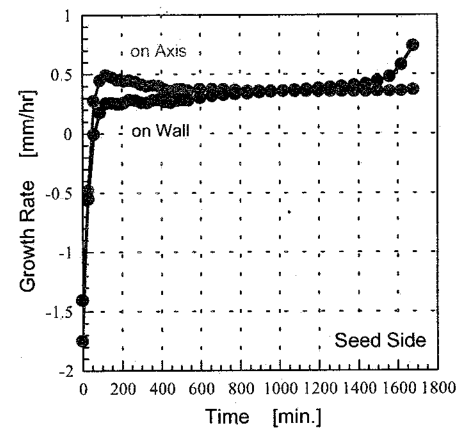

(c) 10^{-4} *g*

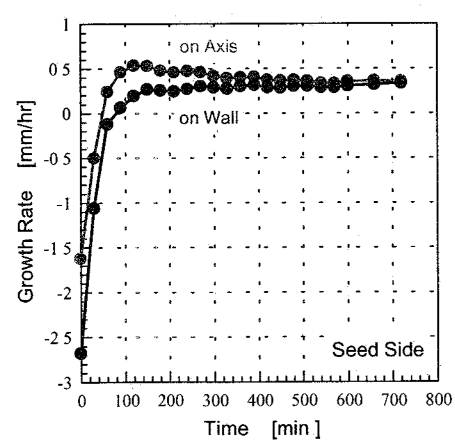

(d) 10^{-2} *g*

Fig. 12 Time Evolutions of Growth Rate at Seed Side (*Cont.*)

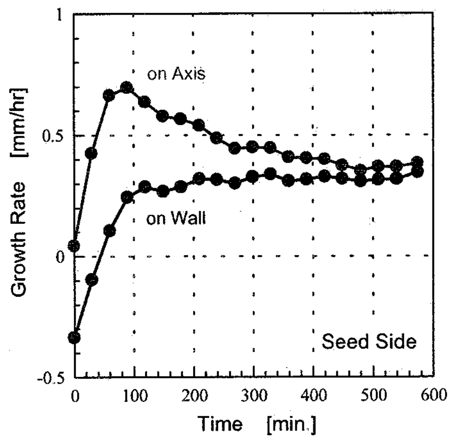

(e) 10^{-1} *g*

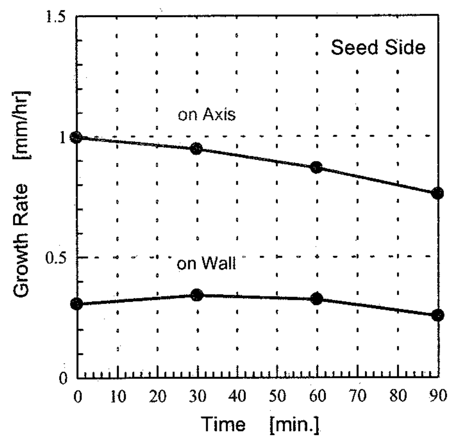

(f) 1 *g*

Fig. 12 Time Evolutions of Growth Rate at Seed Side

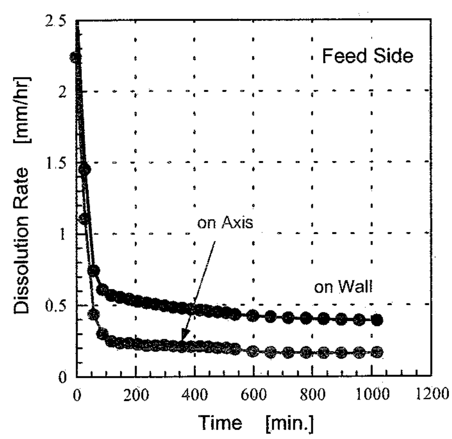

(a) 0 *g*

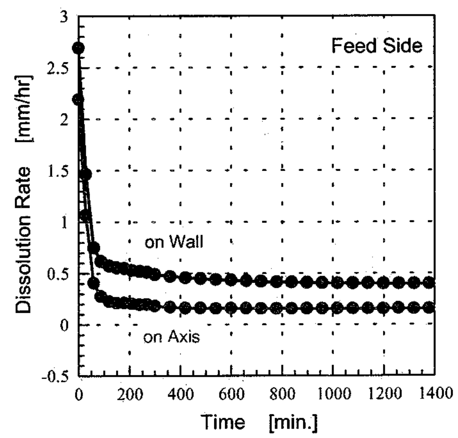

(b) 10^{-5} *g*

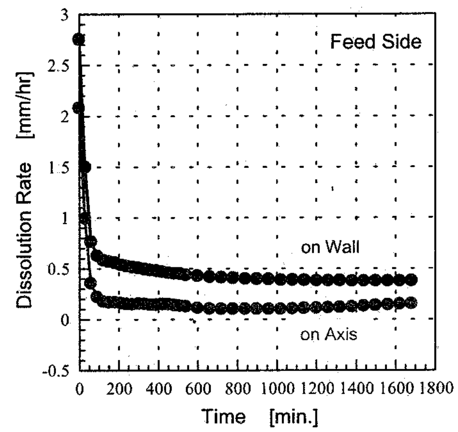

(c) 10^{-4} *g*

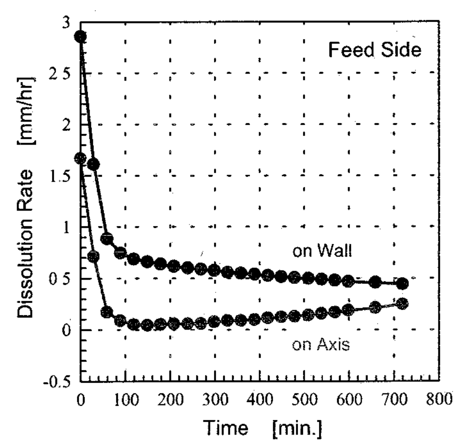

(d) 10^{-2} *g*

Fig. 13 Time Evolutions of Dissolution Rate at Feed Side (*Cont.*)